DOI: 10.1002/chem.201001106

Control of Enantioselectivity with Flexible Biaryl Axes: Terpene-Based Alkylzinc Catalysts in Enantioselective Dialkylzinc Additions

Matthias Leven, Nils E. Schlörer, Jörg M. Neudörfl, and Bernd Goldfuss*[a]

Dedicated to Prof. Paul von Ragué Schleyer to the occasion of his 80th birthday

Abstract: New enantiopure pyridyl alcohols are efficiently accessible through few synthetic steps from commercially available terpenes, that is, (+)-fenchone, (−)-menthone and (−)-verbenone as well as 2,6-diphenylpyridine. These chelating pyridyl alcohols exhibit flexible pyridyl–phenylene axes, which give rise to *P* and *M* conformers. Alkylzincation of the hydroxy groups eliminates equilibria of the conformers and generates alkylzinc complexes with adjusted biaryl axes, as it is demonstrated by NMR studies. These alkylzinc catalysts perform well in the addition of dimethylzinc or diethylzinc to benzaldehyde with yields up to 99% and *ee*'s up to 95%. The adjusted pyridylphenylene conformations in the ligands now control enantioselectivities of the catalysts, which were also analysed by computations at the DFT level.

Keywords: amino alcohols · biaryls · enantioselectivity · homogeneous catalysis · NMR spectroscopy · quantum chemistry · zinc

Introduction

Enantiopure atropisomeric biaryl systems with flexible chiral axes like BINOL (1,1′-bi-2-naphthol) or BINAP (2,2′-bis(diphenylphosphino)-1,1′-binaphthyl) are widely applied in organic syntheses as they provide excellent results as ligands in a broad range of enantioselective catalytic reaction types.[1] Systems that are not atropic isomers, but still contain flexible biaryl axes, might provide adjustable stereogenic units, which then could even further improve the catalyst's performance. An illustrative example is BIFOL **1** (Scheme 1), in which two fenchol units control the sense of conformation of the biaryl axis by intramolecular hydrogen bonds.[2a] A variety of analogous diols, derived from biphenyl with two terpenol frameworks, has been successfully employed in enantioselective catalytic reactions.[2] Reduction of steric crowding and hence increased accessibility to the coordinated metal ion might be achieved by replacement of one of the phenyleneterpenol units by a pyridine group, as in the pyridylphenylene fenchol **2** (Scheme 1).

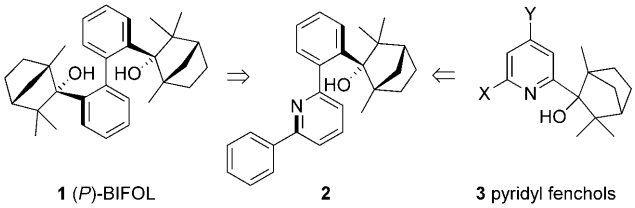

1 (*P*)-BIFOL **2** **3** pyridyl fenchols

Scheme 1. Pyridyl phenylene fenchol **2** as an improved combination of BIFOL **1** and pyridyl fenchols **3**.

Chiral fenchone-based pyridine ligands, such as pyridyl fenchols of type **3** (Scheme 1), have been previously employed in catalysts for enantioselective additions of dialkylzincs to aldehydes[3] and as basis for phosphorous ligands in other transition-metal catalyses or in reagents.[4] The phenylpyridylphenylene fenchol **2** and its analogues derived from menthone and verbenone are studied here with respect to their performance in enantioselective alkylzinc additions to benzaldehyde. The effect of the stereogenic pyridylphenylene axis on the structure and selectivity of the catalyst is of special interest in this study.

[a] M. Leven, Dr. N. E. Schlörer, Dr. J. M. Neudörfl, Prof. Dr. B. Goldfuss
Department of Chemistry, Universität zu Köln
Greinstrasse 4, 50939 Köln (Germany)
Fax: (+49) 221-470-5057
E-mail: goldfuss@uni-koeln.de

Supporting information for this article is available on the WWW under http://dx.doi.org/10.1002/chem.201001106.

Results and Discussion

An efficient synthetic route to terpenols based on the 2,6-diphenylpyridine system is the monolithiation of 2,6-diphenylpyridine at the *ortho* position of a phenyl moiety next to the pyridine unit (Scheme 2).[5] Since this particular type of

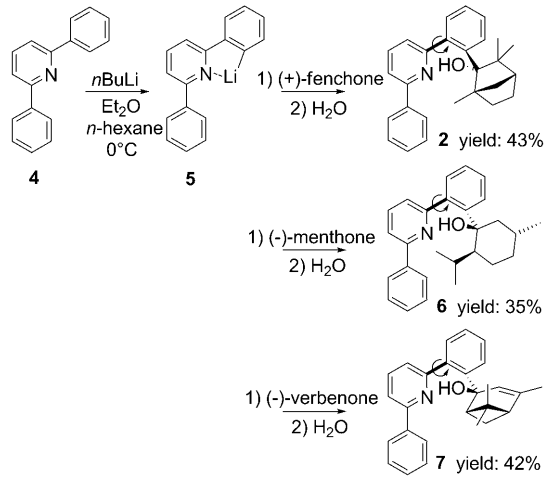

Scheme 2. Synthesis of diphenylpyridine-based terpenols in one-pot reaction sequences. The flexible pyridyl–phenylene axes are shown.

ortho-directed lithiation leads to doubly lithiated products as well,[6a] we had to find a procedure to lithiate the substrate at the appropriate position without competing side reactions (e.g., addition) or double lithiation. Indeed, we found that double lithiation and the competing addition of *n*BuLi to the electron-deficient pyridyl unit (Tschitschibabin reaction[6b]) can be prevented by using inert solvents and absence of de-aggregating ligands at temperatures below 0 °C and 1.2 equivalents of *n*BuLi (previous procedures employed temperatures of 8 °C, diethyl ether and 1.9 equiv *n*BuLi). The subsequent addition of the resulting lithium species to the terpenones can be performed as one-pot reaction (Scheme 2); all side products of the addition, for example, butylterpenols, are easily removable by re-crystallisation.

The one-pot reaction sequences with **5** and the terpenones yield the phenylpyridine terpenols **2**, **6** and **7** as the only stereoisomers. The structure of **2** could be confirmed by an X-ray crystal structure analysis (Figure 1) and confirms the favoured addition of the nucleophile at the *exo*-position of fenchone.[2] (−)-Menthone and (−)-verbenone are known to be attacked from the pro-(*S*) hemisphere, as it is shown in previous additions to these terpenones with other lithium aryls.[2] In agreement with previous work on other systems based on verbenone and menthone, ^{1}H NMR and ^{13}C NMR analytics do not give hints to the presence of further diastereoisomers.[2]

The X-ray crystal structure of **2** shows the flexible, chiral pyridinephenylene axis in a *P* conformation, the torsion

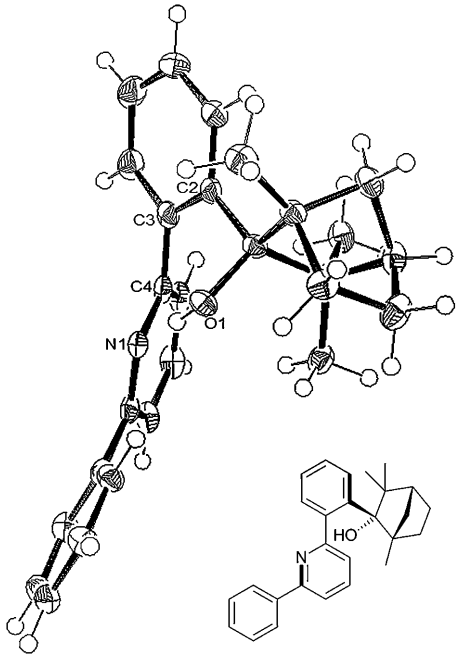

Figure 1. X-ray crystal structure of **2** with *P* conformation of the pyridylphenylene axis (C2-C3-C4-N1); ellipsoides are shown with 50% probability.

angle C2-C3-C4-N1 is 60.8° (Figure 1). Another characteristic feature of aryl fencholates is the rather fixed alignment of the phenylene unit in between the methyl group at C1 and the methylene bridge of the fenchane framework.[2–4] This geometrical preference is also known from many other fencholates (e.g., BIFOL) and guarantees a relatively rigid aryl—fenchane conformation to the backbone of the molecules. A short distance between N1 and O1 of 2.675(2) Å points to a hydrogen bond, the distance between N1 and the hydroxyl hydrogen is 1.80(3) Å (Figure 1).

The equilibrium of the axial conformation of the pyridylphenylene terpenols and the corresponding alkylzinc alkoxides was investigated exemplarily for fencholate **2** by computational DFT studies (Scheme 3) and 2D-NMR experiments, in order to estimate how far the system varies in the conformation of the chiral biaryl axis.

The computational results indicate that the pyridylphenylene conformers **2a** and **2b** are very similar in energy (Scheme 3). The conformer (*P*)-**2b** is slightly favoured by 0.4 kcal mol^{-1}, which is in agreement with the X-ray crystal structure of **2** (Figure 1). The chelating N···H–O hydrogen bond hardly favours one of the conformers. Alkylzincation of **2** drastically changes this conformational equilibrium in the methylzinc alkoxide **8a**/**8b** (Scheme 3): The conformer (*P*)-**8b** now becomes favoured by 5.2 kcal mol^{-1}. Apparently, the equilibrium strongly depends on the ion radius of chelated proton or metal ion, that is, Zn^{2+}. The *P* conformer is favoured $\approx 2\times10^{3}$ times more if Zn^{2+} rather than H^{+} is chelated. As the conformation of the alkylzinc catalyst should be very crucial for its catalytic performance in dialkylzinc additions to aldehydes, the computational studies were com-

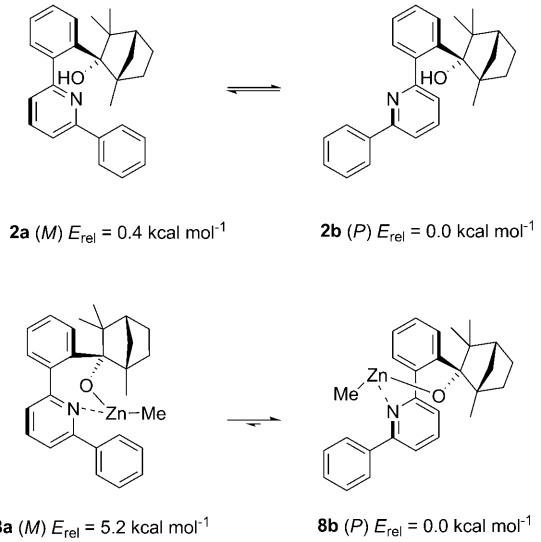

Scheme 3. Preference of conformation of **2** and the corresponding methylzinc alkoxide **8** according to quantum chemical computations in the gas phase, E_{rel} with BP86/SVP + ZPE.

bined with 2D-NMR experiments under catalytic conditions.[7]

The zinc alkoxide **8** could only be detected in the *P* conformation by H,H-NOESY. NOE contacts of the methyl groups 19 and 20 with the pyridine H9 atom (Figure 2) are characteristic for the *P* conformation. There are no visible contacts of methyl group 15 to the pyridine unit, which would be expected for the *M* conformation. The zinc-free pyridylphenylene terpenol **2** on the other hand exhibits NOE contacts for *P* and *M* conformations, in agreement with a fast conformational equilibrium for the rotation around the chiral pyridylphenylene axis. This result is in good agreement with the gas-phase quantum chemical calculations (Scheme 3).

Addition of dialkylzincs to benzaldehyde catalysed by alkylzinc complexes corresponding to 2, 6 and 7: The pyridylphenylene terpenols **2**, **6** and **7** (Scheme 2) were tested as precatalysts in the enantioselective addition of dialkylzinc reagents to benzaldehyde with dimethylzinc and diethylzinc (Scheme 4, Table 1).[8] The reactions were carried out at 0 °C in toluene in the presence of 5 mol % of chiral pyridylphenylene terpenol **2**, **6** or **7**. Taking into account the theoretical results concerning the equilibrium states of the biaryl axes (Scheme 3), we decided to equilibrate each mixture of pyridylphenylene terpenol and dialkylzinc for 30 min at room

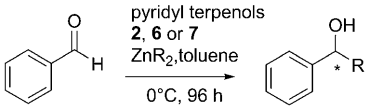

Scheme 4. Pyridylphenylene terpenol catalysed addition of dialkylzinc to benzaldehyde, R = Me, Et.

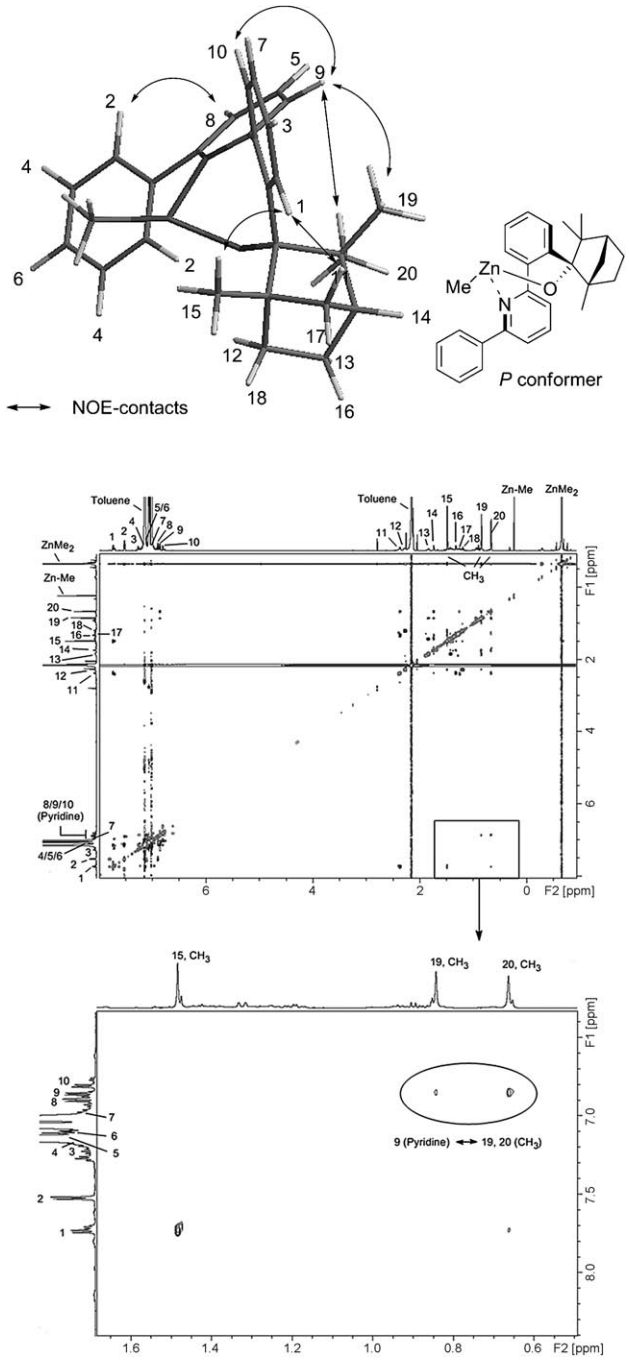

Figure 2. H,H-NOE contacts of the fenchane framework with the pyridine unit confirm *P* conformation for the zinc alkoxide **8b** under catalytic conditions. The positions of the crucial pyridine hydrogen atoms were explicitly confirmed by N,H-correlated spectra. The terpene framework could be characterised by H,H- and H,C-correlated NMR combined with H,H-NOESY. (Spectrum: zinc alkoxide **8b**, H, H NOESY, 600 MHz, T = 0 °C, [D_8]toluene, t_{mix} = 700 ms/structure: computed with BP86/SVP).

temperature to let the stable catalyst conformation form, before benzaldehyde was added at 0 °C.

The yields obtained from the catalytic reactions are all close to total conversion after 96 h (Table 1). While the fencholate **2** reaches enantiomeric exesses (*ee*) up to 95 %, the

Table 1. Pyridyl terpenol screening by the addition of dialkylzinc to benzaldehyde.

Ligand	Dialkylzinc	Yield [%][a]	*ee* [%][b]	Enantiomer
2	Me_2Zn	99	95	*R*
2	Et_2Zn	95	92	*R*
6	Me_2Zn	99	87	*S*
6	Et_2Zn	94	68	*S*
7	Me_2Zn	97	53	*R*
7	Et_2Zn	99	24	*R*

[a] Isolated yields (average results of two reactions). [b] *ee* determined by chiral HPLC/chiracel OD-H, confirmed by use of a racemic reference/ average of two reactions.

Table 2. Qualitative comparisons of diethylzinc additions to benzaldehyde with fencholate catalysts.

Fenchol	Yield [%] (reaction time [h])	*ee* [%]	chelate ring size
3a[3e]	81 (24)	59	5
9a[3b]	99 (24)	64	6
10a X = H[3b]	57 (24)	73	7
10a X = $SiMe_3$[3b]	79 (24)	93	7
2	95 (96)	92	7

mentholate **6** and the verbenolate **7** achieve only up to 87 and 53% *ee*, respectively (Table 1). Surprisingly, the catalytic reactions are more enantioselective for dimethylzinc than for diethylzinc with **2** and **6**. The relatively high enantioselectivity of catalysts based on **2** agrees with the rigid fenchane framework with fixed aryl fencholate backbone.[2]

Comparison of 2 with other fencholates without axial chirality: Other pyridyl fencholates and amino fencholates, which have already been tested in the alkylzinc reaction are compared with **2** in Scheme 5 and Table 2.[3]

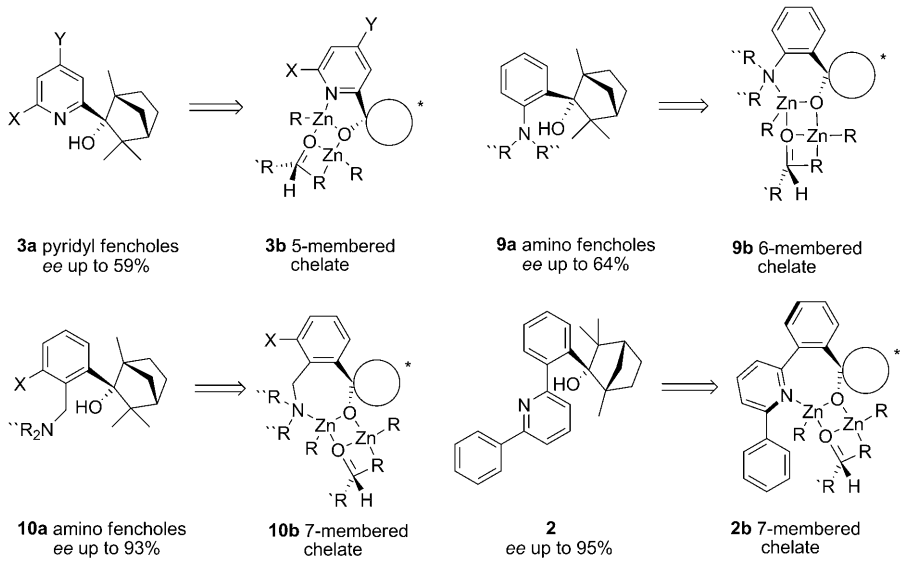

Scheme 5. Various amino alcohols based on fenchones and corresponding transition structures, arranged by the size of the ring that is formed by the zinc alkoxide chelate. The number of chelate ring atoms is compared to the obtained enantiomeric excesses.

A comparison with previously applied fenchols (Table 2, Scheme 5) shows, that the enantiomeric excesses obtained by the different systems in dialkylzinc additions are correlated to the number of ring members involved in the chelate ring of the corresponding alkylzinc alkoxide catalyst: the larger the chelate ring size, the higher the enantioselectivity (Table 2). This might be due to increased steric repulsions of the aldehyde substrate with the fenchane framework with more voluminous ring structures, that is, larger chelate ring sizes.

As the ligands based on 2,6-diphenylpyridine, for example, **2**, shield the zinc ion efficiently with the *ortho*-phenyl group at the pyridine unit, self aggregation and dimerisation of the alkylzinc fencholate catalyst is suppressed.[3] Hence, the higher amount of active monomeric catalyst gives rise to higher reactivities compared to other fencholates (Table 2).

Computational investigations of the addition of dimethylzinc to benzaldehyde catalysed by fencholate 8b: Computational transition structure analyses employing density functional theory show how the structures of the ligands control the enantioselectivities of the corresponding catalysts. From computations of the isolated catalyst **8** (Scheme 3) as well as NMR studies (Figure 2), only the more stable conformer (*P*)-**8b** is considered as active catalyst. In agreement with previous computations,[3,8] the *anti*-transition structures with *anti*-aligned passive alkylzinc groups are more stable than the *syn* species (Tables 2 and 3).[10]

The energetically most favoured *anti-pro-R* transition structure **11a** explains the experimentally favoured formation of the *R*-alcoholic product in the synthetic application of **2**, respectively **8b**, with 95% *ee* (Table 1).

Relatively large energetic differences between *syn*- and *anti*-configured transition structures (Table 3) contribute to this enantioselectivity. The repulsive interaction of the aldehyde substrate with the phenyl group of the ligand is more intensive for the *syn* structures **12a/b** (Figure 3). One of the methyl groups of the fenchane unit reaches far towards the six membered folder of the zinc complex so that the *syn*-conformed structures in **12a/b** are squeezed in between the singly substituted phenyl ring and the fenchane unit. As large substituents, that is, the phenyl group of the aldehyde, are more favourable in *exo* rather than *endo* alignments, the

Table 3. Relative energies of the transition structures **11a–12b** with chiral biaryl axes in *P* conformation (catalyst **8b**, observed in experiment).

TS	Configuration	E_{rel}[a] [kcal mol^{-1}]	ν_i [cm^{-1}]
11a	*anti*, *pro-R*	0.0 (0.0[b])	225 (229[b])
11b	*anti*, *pro-S*	3.3 (2.9[b])	239 (241[b])
12a	*syn*, *pro-R*	13.0 (10.8[b])	271 (285[b])
12b	*syn*, *pro-S*	5.5 (4.8[b])	239 (227[b])

[a] BP86/SVP, *ZPE* included. [b] Transition structures without the phenyl group at the pyridine unit.

Table 4. Relative energies of the transition structures corresponding to **11a–12b** with chiral biaryl axes in *M* conformation (catalyst **8a**, not observed in experiment).

TS	Configuration	E_{rel}[a] [kcal mol^{-1}]	ν_i [cm^{-1}]
11a′	*anti*, *pro-R*	1.5	239
11b′	*anti*, *pro-S*	0.0	227
12a′	*syn*, *pro-R*	5.8	235
12b′	*syn*, *pro-S*	9.4	261

[a] BP86/SVP, *ZPE* included. **11b′** is 4.2 kcal mol^{-1} higher in energy then **11a** in Table 3.

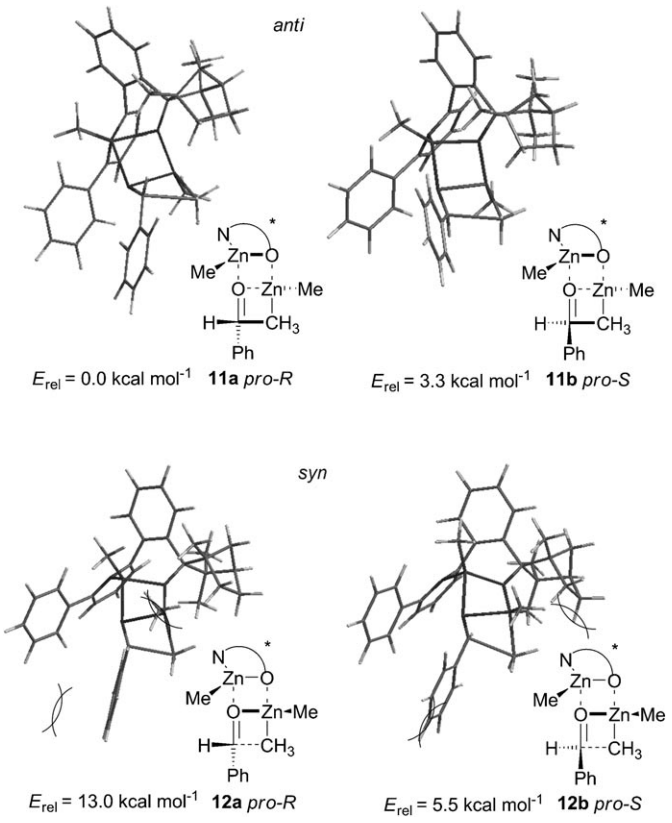

Figure 3. Transition structures for the addition of dimethylzinc to benzaldehyde catalysed by fencholate **8b** (gas phase, BP86/SVP).

anti-pro-R TS **11a** becomes the most favoured transition structure.

The strong influence on the enantioselectivity of the phenyl substituent in the *ortho*-position of the pyridine unit in **8b** becomes apparent from the computed relative energies of **11a**, **11b**, **12a**, **12b** *without* this phenyl substituent (Table 3, energies in parentheses). Without the phenyl group, the energetic differentiations between all transition structures become significantly decreased, which points to the strong influence of the *ortho*-phenyl-substituted pyridine unit on the enantioselectivity of **8b**.

The influence of the orientation of the chiral biaryl axis in **8a/b** on the enantioselectivity of the catalysis was also investigated by transition state calculations. The results in Table 4 indicate that the catalyst **8a** with the biaryl axis in the *M* conformation, which is not observed in experiment, would produce the complementary *S* enantiomer in low enantiomeric ratio, since the *pro-S* TS **11b′** is favoured by only 1.5 kcal mol^{-1}. Transition structures which are corresponding to the catalyst in the *M* conformation are generally upper in energy than TS corresponding to **8b** as it is expected from Scheme 3.

Conclusion

Three new enantiopure terpenols **2**, **6** and **7**, based on (+)-fenchone, (−)-menthone and (−)-verbenone with flexible pyridinephenylene axes have been synthesised. The syntheses include an efficient, newly developed one pot reaction yielding 35–43% product, starting from 2,6-diphenylpyridine. These pyridylphenylene terpenols combine properties of other pyridyl fenchols and biphenyl-based terpenols with flexible biaryl axes previously employed in catalysis. Quantum-chemical computations and 2D-NMR investigations indicate that the stereogenic biaryl axis of **2** is indeed highly flexible, but is tightly adjusted after alkylzincation of **2**, yielding the corresponding alkylzinc catalyst **8b**. Employment of these ligands for the addition of dimethylzinc to benzaldehyde yields the alcoholic product with up to 95% *ee* for **2**, 87% *ee* for **6** and 53% *ee* for **7**. According to DFT studies, the enantioselectivity of the fenchol derivatives **2** and **8b** arises from a large discrimination of *syn*- and *anti*-configured transition structures and the decisive steric hindrance of the phenyl group in *ortho*-position. It was also found, that enantioselectivity would diminish significantly if the conformation of the chiral biaryl axis was not fixed by complexation.

Experimental Section

All reactions were carried out under argon atmosphere using Schlenk technique. Solvents used in chemical conversions were dried by standard methods and distilled under argon prior to use. The enantiomeric excess of the chiral 1-phenylethanols and 1-phenylpropanols were determined by chiral HPLC. We employed the La Chrome elite unit from Hitachi together with the chiral column Chiracel OD-H in 25 cm length. The flow was adjusted to 0,8 mL min^{-1}, the pressure was 32 bar and the detected wavelength $\lambda = 240$ nm. The eluent consisted of 95% *n*-hexanes and 5%

isopropanol. The enantiomers of the alcohols were identified by reference spectra.

Lithiation of 2,6-diphenylpyridine: 2,6-Diphenylpyridine (1 equiv, 500 mg, 2.162 mmol) were degassed in a 150 mL Schlenk tube in vacuum for a period of 30 min. After the Schlenk was purged with argon the solid substance was diluted in a mixture of diethyl ether (20 mL) and *n*-hexanes (20 mL). The mixture was cooled on ice bath and a 1.6 M solution of *n*BuLi in *n*-hexanes (1.2 equiv. 1.62 mL, 2.594 mmol) was added slowly under intensive stirring. The solution was stirred for 8 h at 0 °C and turned slowly to orange while yellow solid material was separated. This crude suspension was used in the subsequent reaction without isolation of the lithio-2,6-diphenylpyridine.

(1*S*,2*S*,4*R*)-1,3,3-trimethyl-2-[(*R*)-2-(6-phenylpyridin-2-yl)phenyl]bicyclo-[2.2.1]heptan-2-ol (2): (+)-Fenchone (1.2 equiv, 0.42 mL, 2.549 mmol) was added to the crude ice-cooled and well-stirred suspension of lithio-2,6-diphenylpyridine. The mixture was stirred for 24 h under thawing of the ice bath. The reaction was quenched by addition of distilled water (10 mL) and the organic phase was separated from the water (separated solid material was added to the organic phase). The aqueous phase was washed diethyl ether (6 mL × 3) and the combined organic phases were evaporated. The remaining solid, light yellow material was transferred into boiling *n*-hexanes (5 mL) and benzene was added dropwise until the solution became homogeneous (ca. 1 mL). Crystallisation at −20 °C yielded 350 mg of colourless crystals (0.923 mmol, 43 %). M.p. 157.8 °C; $[\alpha]_{Na}^{20} = -1781$ ($c = 1$ in toluene); ^{1}H NMR ($CDCl_3$, 300 MHz): $\delta = 0.44$ (s, 3H), 0.65 (s, 3H), 1.12 (m, 1H), 1.32 (m, 2H), 1.39 (s, 3H), 1.66 (m, 2H), 2.38 (m, 1H), 2.48 (m, 1H), 6.13 (s, 1H), 7.28 (m, 3H), 7.37 (m, 1H), 7.48 (m ,3H), 7.73 (d, $J = 7.8$ Hz, 1H), 7.85 (q, $J = 7.8$ Hz, 2H), 8.05 ppm (d, $J = 6.9$ Hz, 2H); ^{13}C NMR ($CDCl_3$, 75.5 MHz): $\delta = 18.88$, 21.71, 24.26, 30.40, 34.36, 41.27, 45.14, 50.70, 54.08, 86.54, 118.70, 124.81, 125.63, 126.60, 127.17, 128.85, 129.18, 133.16, 137.79, 138.42, 141.16, 144.67, 154.88, 163.94 ppm; X-ray crystal data: $C_{27}H_{29}NO$; $M_r = 383.51$ g mol^{-1}; space group: $P2_12_12_1$; $a = 9.6472(6)$, $b = 11.3259(6)$, $c = 18.8724(8)$ Å; $V = 2062.01(2)$ Å^3; $Z = 4$; $\rho = 1.235$ g mL^{-3}; $T = 100(2)$ K; $\lambda = 0.71073$ Å; $\mu = 0.074$ mm^{-1}; total reflections: 9135; unique reflections: 2555; observed: 2072 [$I > 2\sigma(I)$]; parameters refined: 269; $R1 = 0.0371$, $wR2 = 0.0774$; GOF = 1.001; H atoms bound to oxygen were refined, the positions of the H atoms bound to carbon were calculated. CCDC-773286 (**2**) contains the supplementary crystallographic data for this paper. These data can be obtained free of charge from The Cambridge Crystallographic Data Centre via www.ccdc.cam.ac.uk/data_request/cif.

(1*S*,2*S*,5*R*)-2-Isopropyl-5-methyl-1-[2-{(*S*)-6-phenylpyridin-2-yl}phenyl]-cyclohexanol (6): (−)-Menthone (1.2 equiv, 0.45 mL, 2.549 mmol) was added to the crude ice-cooled and well-stirred suspension of lithio-2,6-diphenylpyridine. The mixture was stirred for 24 h under thawing of the ice bath and the deep orange colour turned to light yellow. The reaction was quenched by addition of distilled water (10 mL) and the organic phase was separated from the water. The aqueous phase was washed with diethyl ether (6 mL × 3) and the combined organic phases were evaporated. The remaining solid, light yellow material was transferred into boiling *n*-pentane (10 mL) and benzene was added dropwise until the solution became homogeneous. Crystallisation at −20 °C yielded cotton like solid material which was washed with cold *n*-pentane until the light yellow colour vanished. The organic solution still contained **6**, which could be gained by crystallisation. Yield: 293 mg (0.761 mmol, 35 %); m.p.: 101.6 °C; $[\alpha]_{Na}^{20} = +593$ ($c = 1$ in toluene); ^{1}H NMR ($CDCl_3$, 300 MHz): $\delta = 0.75$ (d, $J = 6.9$ Hz, 3H), 0.78 (d, $J = 6.9$ Hz, 3H), 0.89 (d, $J = 6.3$ Hz, 3H), 1.56 (m, 3H), 1.81 (m, 4H), 2.23 (m, 1H), 2.97 (s, 1H), 7.28 (m, 2H), 7.44 (m, 6H), 7.72 (m, 1H), 7.85 (m, 1H), 8.02 ppm (d, $J = 6.6$ Hz, 2H); ^{13}C NMR ($CDCl_3$, 75.5 MHz): $\delta = 18.79$, 21.55, 22.27, 23.97, 27.34, 28.07, 35.40, 50.50, 53.18, 81.21, 117.87, 122.65, 125.74, 126.95, 127.21, 127.98, 128.63, 129.08, 132.81, 137.89 ppm.

(1*S*,2*S*,5*S*)-4,6,6-Trimethyl-2-[2-{(*S*)-6-phenylpyridin-2-yl}phenyl]bicyclo-[3.1.1]hept-3-en-2-ol (7): (−)-Verbenone (1.2 equiv, 0.40 mL, 2.549 mmol) was added to the crude ice-cooled and well-stirred suspension of lithio-2,6-diphenylpyridine. The mixture was stirred for 24 h under thawing of the ice bath. The reaction was quenched by addition of distilled water (10 mL) and the organic phase was separated from the water. The aqueous phase was washed with diethyl ether (6 mL × 3) and the combined organic phases were evaporated. The remaining solid, light yellow material was transferred into boiling *n*-hexanes (5 mL) and benzene was added dropwise until the solution became homogeneous (ca. 1 mL). Crystallisation at −20 °C yielded 343 mg of white solid material (0.889 mmol, 42 %). M.p. 132.7 °C; $[\alpha]_{Na}^{20} = +325$ ($c = 1$ in toluene); ^{1}H NMR ($CDCl_3$, 300 MHz): $\delta = 1.05$ (s, 3H), 1.15 (s, 4H), 1.76 (s, 3H), 1.91 (dd, $J = 5.1$ Hz, 1H), 2.09 (m, 2H), 5.50 (s, 1H), 7.46 (m, 7H), 7.62 (d, $J = 7.8$ Hz, 1H), 7.78 (d, $J = 7.8$ Hz, 1H), 7.95 (d, $J = 7.8$ Hz, 1H), 7.99 (d, 6.9 Hz, 2H), 8.10 ppm (s, 1H); ^{13}C NMR ($CDCl_3$, 75.5 MHz): $\delta = 23.10$, 23.40, 27.67, 34.22, 43.50, 47.10, 50.31, 79.23, 119.33, 121.72, 123.70, 127.15, 128.29, 128.43, 128.99, 133.00, 138.38, 138.63, 138.72, 145.39, 146.65, 155.71, 162.13 ppm.

Addition of dimethylzinc to benzaldehyde:[9] Pyridylphenylene terpenol (0.074 mmol, 5 mol %; **2**: 28 mg; **6**: 29 mg; **7**: 28 mg) was degassed in vacuum for a period of 10 min. The substance was dissolved in toluene (6 mL) and a solution of 2.0 M dimethylzinc in toluene (1.8 mL, 3.6 mmol) was added at 0 °C. The ice bath was removed and the catalyst was equilibrated for 30 min at room temperature. The mixture was cooled on the ice bath again and distilled benzaldehyde (0.15 mL) was added. The colourless solution was kept at 0 °C for 4 days and the reaction was subsequently quenched with saturated NH_4Cl solution (5 mL). The organic phase was diluted with diethyl ether (10 mL) and rapidly washed with 10 % HCl (5 mL) and three portions a distilled water (5 mL). The combined aqueous phases were washed with diethyl ether (5 mL × 3) and the resulting combined organic phases were evaporated. The resulting colourless oil was purified by column chromatography (*n*-hexanes/ethylacetate 3:1, 70 g SiO_2, $R_f = 0.41$). The enantiomeric ratio was determined by chiral HPLC. ((*R*)-1-phenylethanol: 11.2 min; (*S*)-1-phenylethanol: 13.6 min).

Addition of diethylzinc to benzaldehyde:[8] Pyridylphenylene terpenol (0.074 mmol, 5 mol %; **2**: 28 mg; **6**: 29 mg; **7**: 28 mg) was degassed in vacuum for a period of 10 min. The substance was dissolved in toluene (6 mL) and a solution of 1.0 M diethylzinc in *n*-hexanes (2.4 mL, 2.4 mmol) was added at 0 °C. The ice bath was removed and the catalyst was equilibrated for 30 min at room temperature. The mixture was cooled on the ice bath again and distilled benzaldehyde (0.15 mL) was added. The nearly colourless solution was kept at 0 °C for 4 days and the reaction was subsequently quenched with saturated NH_4Cl solution (5 mL). The organic phase was diluted with diethyl ether (10 mL) and rapidly washed with 10 % HCl (5 mL) and three portions a distilled water (5 mL). The combined aqueous phases were washed with diethyl ether (5 mL × 3) and the resulting combined organic phases were evaporated. The resulting oil was purified by column chromatography (*n*-hexanes/ethylacetate 3:1, 70 g SiO_2, $R_f = 0{,}45$). The enantiomeric ratio was determined by chiral HPLC. ((*R*)-1-phenylpropanol: 10.2 min; (*S*)-1-phenylethanol: 12.1 min).

NMR spectroscopy: Deuterated solvents were purchased from Eurisо-Top (France) ([D_8]toluene) and Deutero GmbH, Kastellaun (Germany) ([D]chloroform). [D]Chloroform was dried over molecular sieves and [D_8]toluene was stored over sodium-lead alloy. NMR spectra for characterisation of compounds where recorded with a Bruker DPX 300 spectrometer (^{1}H frequency 300.13 MHz). 2D NMR and one-dimensional high-resolution spectra for conformation analysis of the catalytically active system were recorded on a Bruker AVANCE II 600 spectrometer (^{1}H frequency 600.20 MHz) by using a triple resonance Z gradient probe and processed using TopSpin 2.1 software (Bruker inc.). The temperature was calibrated with a 100 % methanol sample. NMR samples were prepared by dissolving degassed **2** (5 mg) in [D_8]toluene (500 μL) in a vacuum dried NMR tube to give solutions of about 0.05 mol L^{-1}. Dimethylzinc in toluene was added (0.03 mL, 56 mmol, 4.6 equiv) under argon atmosphere in a Schlenk tube.

Computational details: All theoretical calculations were performed with the program package TURBOMOLE-5.10. The employed density functional was BP86 with the current grid size m3 combined with the contracted SVP-basis-set from Aldrich et al. The resolution of identity approximation for two-electron integral evaluation was used. All stationary points were fully optimised and confirmed by separate analytical fre-

quency calculations. Transition structures were optimised with quasi-Newton-Raphson methods by using the Powell-update algorithm for hessian matrix approximation (analytical frequency calculation subsequent). Absolute energies were zero point corrected with the vibrational information recieved from harmonical analytical frequency calculations.

Acknowledgements

We are grateful to the Fonds der Chemischen Industrie for financial support. We especially thank the Deutsche Forschungsgemeinschaft (DFG) for funding (GO-930/9-1) as well as Bayer AG, BASF AG, Wacker AG, Evonic AG, Raschig GmbH, Symrise GmbH, Solvay GmbH and OMG group for generous support.

[1] a) K. Schober, E. Hartmann, H. Zhang, R. M. Gschwind, *Angew. Chem.* **2010**, *122*, 2855–2859; *Angew. Chem. Int. Ed.* **2010**, *49*, 2794–2797; b) J. M. Brunel, *Chem. Rev.* **2005**, *105*, 857–897; c) M. Shibasaki, H. Sasai, T. Arai, *Angew. Chem.* **1997**, *109*, 1290–1311; *Angew. Chem. Int. Ed. Engl.* **1997**, *36*, 1236–1256; d) H. Sasai, T. Arai, Y. Satow, K. N. Houk, *J. Am. Chem. Soc.* **1995**, *117*, 6194–6198; e) G. J. Grant, J. A. Pool, D. Van Derveer, *Dalton Trans.* **2003**, 3981–3984; f) M. Shibasaki, N. Yoshikawa, *Chem. Rev.* **2002**, *102*, 2187; g) J. Oppenheimer, R. P. Hsung, R. Figueroa, W. L. Johnsen, *Org. Lett.* **2007**, *9*, 3969–3972; h) U. Matteoli, V. Beghetto, C. Schiavon, A. Scrivanti, G. Menchi, *Tetrahedron: Asymmetry* **1997**, *8*, 1403–1409.

[2] a) B. Goldfuss, F. Rominger, *Tetrahedron* **2000**, *56*, 881–884; b) Y. Alpagut, B. Goldfuss, J. Neudörfl, *Beilstein J. Org. Chem.* **2008**, *4*, 25; c) B. Goldfuss, F. Soki, J. Neudörfl, *J. Organomet. Chem.* **2008**, *693*, 2139–2146; d) B. Goldfuss, T. Kop-Weiershausen, J. Lex, J. Neudörfl, *J. Org. Chem.* **2005**, *70*, 1; e) B. Goldfuss, T. Löschmann, F. Romiger, *Chem. Eur. J.* **2001**, *7*, 2028–2033; f) V. Dimitrov, G. Dobrikov, M. Genov, *Tetrahedron: Asymmetry* **2001**, *12*, 1323–1329; g) I. Philipova, V. Dimitrov, S. Simova, *Tetrahedron: Asymmetry* **1999**, *10*, 1381–1391.

[3] a) M. Steigelmann, Y. Nisar, F. Rominger, B. Goldfuss, *Chem. Eur. J.* **2002**, *8*, 5211–5218; b) B. Goldfuss, M. Steigelmann, S. I. Khan, K. N. Houk, *J. Org. Chem.* **2000**, *65*, 77- 82; c) B. Goldfuss, M. Steigelmann, F. Romiger, *Eur. J. Org. Chem.* **2000**, 1785–1792; d) W. A. Herrmann, J. J. Haider, J. Fridgen, G. M. Lobmaier, M. Spiegler, *J. Organomet. Chem.* **2000**, *603*, 69–79; e) M. Steigelmann, Dissertation, Universität Heidelberg (Germany), **2002**, p. 96.

[4] a) B. Goldfuss, T. Löschmann, T. Kop-Weiershausen, J. Neudörfl, F. Rominger, *Beilstein J. Org. Chem.* **2006**, *2*, 7; b) D. A. Lange, J. M. Neudörfl, B. Goldfuss, *Tetrahedron* **2006**, *62*, 3704–3709; c) B. Goldfuss, F. Soki, J. Neudörfl, *Tetrahedron* **2005**, *61*, 10449–10453; d) B. Goldfuss, *Synthesis* **2005**, 2271–2280; e) B. Goldfuss, M. Steigelmann, T. Löschmann, G. Schilling, F. Romiger, *Chem. Eur. J.* **2005**, *11*, 4019–4023; f) B. Goldfuss, T. Löschmann, F. Romiger, *Chem. Eur. J.* **2004**, *10*, 5422–5431; g) B. Goldfuss, M. Steigelmann, F. Romiger, *Angew. Chem.* **2000**, *112*, 4299–4302; *Angew. Chem. Int. Ed.* **2000**, *39*, 4133–4136.

[5] a) V. Snieckus, *Chem. Rev.* **1990**, *90*, 879–933; b) L. Brandsma, *Preparative Polar Organometallic Chemistry, Vol. 2*, Springer, Berlin, **1987**, pp. 127–143; c) F. Reed, *Spec. Chem. Mag.* **1994**, *14*, 18; d) K. Shankaran, V. Snieckus, *J. Org. Chem.* **1984**, *49*, 5022; e) R. J. Chongau, M. A. Siddiqui, V. Snieckus, *Tetrahedron Lett.* **1986**, *27*, 5323.

[6] a) C. Corinoley-Deuschel, T. Ward, A. von Zelewski, *Helv. Chim. Acta* **1988**, *71*, 130–133; b) K. Ziegler, H. Zeiser, *Ber. Dtsch. Chem. Ges.* **1930**, *63*, 1847.

[7] For recent NMR studies on metal catalysts, see: a) K. Schober, E. Hartmann, H. Zhang, R. M. Gschwind, *Angew. Chem.* **2010**, *122*, 2855-2859; *Angew. Chem. Int. Ed.* **2010**, *49*, 2794-2797; b) T. Thaler, B. Haag, A. Gavryushin, K. Schober, E. Hartmann, R. M. Gschwind, H. Zipse, P. Mayer, P. Knochel, *Nat. Chem.* **2010**, *2*, 125–130.

[8] a) R. Noyori, M. Kitamura, *Angew. Chem.* **1991**, *103*, 34–55; *Angew. Chem. Int. Ed. Engl.* **1991**, *30*, 49–69; b) L. Pu, H. Yu, *Chem. Rev.* **2001**, *101*, 757; c) K. Soai, S. Niwa, *Chem. Rev.* **1992**, *92*, 833; d) K. Yoshida, T. Toyoshima, N. Akashi, T. Imamoto, A. Yanagisawa, *Chem. Commun.* **2009**, 2923–2925; e) R. Martínez, L. Zoli, P. G. Cozzi, D. J. Ramon, M. Yus, *Tetrahedron: Asymmetry* **2008**, *19*, 2600–2607; f) J. K. Nelson, B. Twamley, T. J. Villalobos, N. R. Natale, *Tetrahedron Lett.* **2008**, *49*, 5957–5960; g) I. Sato, N. Asakura, T. Iwashita, *Tetrahedron: Asymmetry* **2007**, *18*, 2638–2642; h) C. Bolm, F. Schmidt, L. Zani, *Tetrahedron: Asymmetry* **2005**, *16*, 1367–1376; i) C. Bolm, L. Zani, J. Rudolph and I. Schiffers, *Synthesis* **2004**, 2173–2180.

[9] a) L. Pisani, S. Superchi, *Tetrahedron: Asymmetry* **2008**, *19*, 1784–1789; b) M. P. Krzeminski, B. Singaram, *J. Org. Chem.* **2009**, *74*, 2337–2343.

[10] a) M. Kitamura, H. Oka, R. Noyori, *Tetrahedron* **1999**, *55*, 3605; b) M. Yamakawa, R. Noyori, *Organometallics* **1999**, *18*, 128; c) B. Goldfuss, K. N. Houk, *J. Org. Chem.* **1998**, *63*, 8998–9006.

Received: April 27, 2010
Published online: October 6, 2010

